

Article

# Comparative Analysis of Hybrid Maximum Power Point Tracking Algorithms Using Voltage Scanning and Perturb and Observe Methods for Photovoltaic Systems under Partial Shading Conditions

Musa Yilmaz <sup>1,2</sup> 

<sup>1</sup> Center for Environmental Research and Technology, Bourns College of Engineering, University of California at Riverside, Riverside, CA 92521, USA; musay@ucr.edu

<sup>2</sup> Department of Electrical and Electronics Engineering, Batman University, 72100 Batman, Turkey

**Abstract:** Partial shading significantly affects the performance of photovoltaic (PV) power systems, rendering traditional maximum power point tracking (MPPT) methods ineffective. This study proposes a novel hybrid MPPT algorithm integrating voltage scanning and modified Perturb and Observe (P&O) techniques to overcome the limitations posed by partial shading. This algorithm has a simple structure and does not require panel information such as the number of panels or voltage due to its voltage scanning feature. To test the proposed algorithm, a grid-connected PV power system with a power of 252.6 kW was created in the MATLAB/Simulink environment. In this power system, six different PS conditions, containing quite challenging situations, were listed in three different scenarios and simulated. The proposed algorithm was compared with the voltage scanning and P&O and voltage scanning and variable-step P&O methods. It was observed that the proposed algorithm has lower power fluctuations compared to the other two traditional methods. Additionally, this algorithm managed to achieve higher efficiency than the other methods in some cases.



**Citation:** Yilmaz, M. Comparative Analysis of Hybrid Maximum Power Point Tracking Algorithms Using Voltage Scanning and Perturb and Observe Methods for Photovoltaic Systems under Partial Shading Conditions. *Sustainability* **2024**, *16*, 4199. <https://doi.org/10.3390/su16104199>

Academic Editors: Mohamed A. Mohamed, David Alfonso-Solar and Carlos Vargas-Salgado

Received: 23 March 2024

Revised: 15 May 2024

Accepted: 15 May 2024

Published: 16 May 2024



**Copyright:** © 2024 by the author. Licensee MDPI, Basel, Switzerland. This article is an open access article distributed under the terms and conditions of the Creative Commons Attribution (CC BY) license (<https://creativecommons.org/licenses/by/4.0/>).

**Keywords:** MPPT (maximum power point tracking); PV systems; partial shading; hybrid algorithms; efficiency analysis

## 1. Introduction

Due to factors such as global warming, the depletion of fossil fuels, and environmental pollution, the importance of renewable energy sources is increasing. Solar energy holds a significant place among these renewable energy sources. The efficiencies of solar panels are quite low. Therefore, maximum power point tracking (MPPT) algorithms have been developed to obtain maximum efficiency from solar panels [1,2]. Perturb and Observe (P&O) and voltage scanning (VSC) are two primary methods employed in maximum power point tracking (MPPT) for photovoltaic (PV) systems. P&O operates by perturbing either the voltage or current of the PV system and observing the resulting change in power output. This method is straightforward to implement and requires minimal computational resources, making it suitable for various PV system applications. It relies on direct measurements of voltage and current, allowing for easy integration into standard PV system components. P&O exhibits a fast response time, adjusting the operating point quickly to changes in environmental conditions. However, it often suffers from overshooting and oscillation, especially under rapidly changing irradiance conditions.

On the other hand, VSC operates by systematically scanning the voltage range of the PV system to determine the point of maximum power output. Unlike P&O, VSC does not involve perturbing the operating point; instead, it directly measures the power output at each voltage level. VSC algorithms are relatively simple in concept and implementation, making them suitable for real-time control in PV systems. They can adapt to

varying environmental conditions without the risk of overshooting or oscillation, resulting in robust performance in dynamic environments. Moreover, VSC does not require direct measurements of current, simplifying hardware requirements and reducing cost. However, VSC algorithms may have a slower response time since they systematically scan the entire voltage range to find the MPP. A considerable number of MPPT algorithms have been developed in the literature. Among them, the oldest ones are the Perturb and Observe (P&O) and Incremental Conductance (InC) algorithms [3]. However, these algorithms are insufficient to capture the maximum power under partial shading conditions (PSC) in photovoltaic power systems. Therefore, modified P&O and InC algorithms, hybrid algorithms, or optimization-based intelligent algorithms are used [4]. Although the currency of intelligent algorithms has increased in recent years, their processing complexity is high, and difficulties are encountered in application. Therefore, studies on modified traditional algorithms are still ongoing today.

Pandey and colleagues developed a new algorithm by making the duty period used in the traditional P&O algorithm variable in size, thus increasing the speed in capturing maximum power and minimizing the drift phenomenon [5]. In a similar study, Ahmed and colleagues modified the P&O algorithm, reducing the oscillations in steady state and increasing the power tracking efficiency according to EN50530 dynamic radiation tests [6]. Li and colleagues combined the algorithm with an adaptive control algorithm, thus obtaining a faster-acting algorithm [7]. Ahmed and colleagues developed an algorithm that operates with higher efficiency by improving the traditional P&O algorithm [8]. Abdelsalam and colleagues developed a P&O algorithm that reduces steady-state oscillations [9]. Killi and colleagues proposed a P&O algorithm that eliminates the drift phenomenon and demonstrated the superiority of their algorithm with experimental results [10]. Zhu and colleagues developed a new algorithm that operates faster and can generate power with low oscillation by updating the traditional P&O algorithm [11]. Belkaid and colleagues developed a new MPPT algorithm that operates with higher efficiency by improving the traditional P&O algorithm. They demonstrated their superiority by testing their proposed algorithm according to standards [12,13].

The traditional P&O algorithm operates with very low efficiency under partial shading conditions. Therefore, various modified P&O algorithms are effective under partial shading conditions. Ahmed and colleagues developed a P&O algorithm that can operate effectively under partial shading conditions and compared it with current algorithms [14,15]. In recent years, hybrid MPPT algorithms, formed by combining the P&O method with other methods, are also extensively used. Ayad and colleagues developed a high-performance algorithm with low oscillation by using an artificial neural network (ANN) together with P&O algorithms [16]. Restrepo and colleagues proposed a new MPPT algorithm that can operate with high performance under both uniform sunlight and partial shading conditions. Their proposed algorithm is a hybrid MPPT algorithm consisting of artificial bee colony optimization and the P&O algorithm [17]. Hua and colleagues similarly proposed an MPPT algorithm consisting of a genetic algorithm and P&O algorithms [18]. Farzaneh developed a hybrid MPPT algorithm combining modified firefly algorithm-based ANFIS and P&O methods [19]. Çelik and Teke developed a hybrid MPPT algorithm consisting of ANN and P&O methods that can be used in grid-connected PV systems [20]. Similarly, studies on different combinations like Learning Automata and P&O [21], grey wolf optimization and P&O [22], ANN and P&O [23], P&O and particle swarm optimization [24], Fractional Short-Circuit Current Measurement and P&O [25], particle swarm optimization -P&O [26], salp swarm optimization and P&O [27,28] are found in the literature. Voltage scanning (VSC) and voltage segmentation algorithms are especially used in PV systems operating under partial shading conditions [29]. Başoğlu, in two different studies, developed duty cycle scanning and voltage scanning algorithms, obtaining maximum power from the PV power system at the module level [30,31]. Jatly and colleagues developed a new MPPT method that operates with high efficiency under rapidly changing radiation conditions by performing both voltage and current scanning [32]. Kesilmiş and colleagues developed

a high-efficiency MPPT method under partial shading conditions by detecting voltage bends with an algorithm and identifying voltage segments [33]. In a very recent study, an adaptive voltage scanning method was developed, creating a high-performance MPPT method that can operate under partial shading conditions [34]. Ostadrahimi and colleagues developed a scanning-based algorithm that operates faster than the traditional 0.8Voc voltage segmentation algorithm by developing a spline MPPT method [35]. Lyden and colleagues developed a high-efficiency MPPT algorithm by combining the voltage scanning-based Simulated Annealing method with the P&O method [36].

Zhang and colleagues designed a high-efficiency hybrid MPPT algorithm by combining a voltage scanning-based MPPT algorithm with the ANN method and demonstrated the results in a simulation environment [37]. In another study, the algorithm was made to work faster by skipping certain voltage regions while scanning, preventing the algorithm from scanning unnecessary areas [38].

When the literature is generally reviewed, it is seen that hybrid MPPT algorithms operate with high performance. However, hybrid MPPT algorithms are generally used together with optimization algorithms, so their processing complexity is at a high level. On the other hand, hybrid MPPT algorithms used together with the voltage segmentation method require information such as panel voltage and the number of panels connected in series. Changes in the catalog Voc voltages of panels over time reduce the efficiency of these methods in the long run.

In this study, a VSC-modified P&O-based algorithm was developed for a grid-connected PV power system. The proposed algorithm operates with high performance under partial shading conditions. The most important features of the algorithm are its quite simple structure and obtaining low oscillation in steady state using modified P&O. On the other hand, there is no need for information such as the number of panels or voltage in the proposed method. A PV power system with 609 panels, consisting of 7 series panels and 87 parallel strings, with a power of 252.6 kW, was created in the MATLAB/Simulink environment. In the simulation, power, current, and voltage information were obtained by running six different partial shading conditions in three different scenarios. The proposed VSC-modified P&O (VSC-M\_P&O) [12] algorithm was compared with hybrid MPPT methods combining the VSC method with the P&O method (VSC-P&O) and the VSC method with variable-step P&O (VSC-VS\_P&O) [5]. The obtained results are presented graphically and in tables.

## 2. Grid-Connected PV System and Partial Shading

In this study, to test the performance of the proposed method, a PV power system with a power of 252.6 kW was created. This system consists of a total of 609 panels, with 87 parallel arrays and 7 series-connected panels in each array. A PV cell model consists of a well-known diode, a current source, and two resistors. The output current produced here is expressed as seen in Equations (1) to (3) [1,34].

$$I = I_{PV} - I_D - I_{Rp} \quad (1)$$

$$I = I_{PV} - I_0 \left[ \exp\left(\frac{V + R_s I}{a}\right) - 1 \right] - \frac{V + R_s I}{R_p} \quad (2)$$

$$a = \frac{N_s n k T}{q} \quad (3)$$

where  $I_0$  refers to the reverse saturation current or leakage current of the diode, which is a crucial parameter in determining the performance of the photovoltaic (PV) cell. The factor  $a$ , known as the ideality factor, typically ranges between 1 and 2, and provides insight into the recombination processes occurring within the diode.  $N_s$  denotes the number of series-connected cells in the PV module, which directly affects the overall voltage output of the system. The diode ideality constant  $n$  is a dimensionless parameter that further characterizes the diode's behavior under different conditions.

The Boltzmann constant  $k$  ( $1.3806503 \times 10^{-23}$  J/K) is a fundamental physical constant that relates the average kinetic energy of particles in a gas with the temperature of the gas, playing a significant role in the statistical mechanics of particles. The temperature  $T$  of the cell, measured in Kelvin, is a critical factor as it influences the thermal agitation of charge carriers, thereby affecting the current and voltage characteristics of the PV cell. The electron charge  $q$  ( $1.60217646 \times 10^{-19}$  C) is a fundamental charge of an electron, essential for calculations involving electrical phenomena in semiconductor devices.

Equation (4) specifically describes the current generated by the PV cell as a function of the incident light, considering all the aforementioned parameters. This light-generated current is pivotal for the conversion of solar energy into electrical energy, as it directly translates the photonic energy absorbed by the cell into a usable electric current. The interplay between these variables defines the efficiency and effectiveness of the PV cell in harnessing solar power. The precise understanding and calculation of these parameters are essential for optimizing the design and functionality of PV systems to ensure maximum energy output and reliability.

$$I_{PV} = (I_{PV,n} + K_I(T - T_n)) \frac{G}{G_n} \quad (4)$$

where  $I_{PV,n}$  refers to the current generated by the photovoltaic (PV) cell under standard conditions of 25 °C and 1000 W/m<sup>2</sup> irradiance.  $T_n$  represents the nominal temperature in Kelvin, crucial for understanding the PV cell's thermal behavior.  $G$  denotes the actual radiation on the panel surface (W/m<sup>2</sup>), directly influencing the electrical output. Conversely,  $G_n$  represents the nominal radiation value (W/m<sup>2</sup>) under standard test conditions.

Equation (5) describes the diode's saturation current ( $I_0$ ), a fundamental parameter affecting the diode's current–voltage relationship.

$I_0$  plays a critical role in determining the PV cell's behavior, influencing efficiency and performance under various conditions. Understanding these parameters helps in predicting and optimizing the energy output of PV systems, ensuring efficient operation under real-world conditions.

$$I_0 = \frac{I_{SC,n} + K_I(T - T_n)}{\exp\left(\frac{V_{OC,n} + K_V(T - T_n)}{a}\right) - 1} \quad (5)$$

where  $I_{SC,n}$  is the nominal short-circuit current,  $V_{OC,n}$  is the nominal open-circuit voltage,  $K_I$  is the current coefficient, and  $K_V$  is the voltage coefficient. The data for the panels used in the PV power system can be seen in Table 1.

**Table 1.** SunPower SPR-415E-WHT-D parameters.

Symbol	Quantity	Values	
$P_{MPP}$	Maximum power at MPP	414.801	W
$V_{MPP}$	MPP voltage	72.9	V
$I_{MPP}$	MPP current	5.69	A
$V_{OC}$	Open-circuit voltage	85.3	V
$I_{SC}$	Short-circuit current	6.09	A
$T_C$	Temp. coefficient of Voc	−0.229	%/°C
$T_C$	Temp. coefficient of Isc	0.030706	%/°C
$R_S$	PV series resistance	0.53711	Ω
$R_P$	PV shunt resistance	419.7781	Ω
$N_{cell}$	Cells per module	128	

The voltage of the PV power system is increased by connecting the panels in series, while the power value of the system is increased by connecting the panels in parallel. The maximum power value that can be obtained from the PV power system is calculated under standard atmospheric conditions (25 °C–1000 W/m<sup>2</sup>). However, the irradiance value may

not always be the same across all panels. The power value generated by the system will change under various shading conditions. Traditional MPPT algorithms are insufficient in calculating the maximum power value under partial shading conditions (PSCs). Therefore, different MPPT algorithms were developed. Figure 1 shows the current, voltage, and power value generated by the first PS event created in the simulated system.

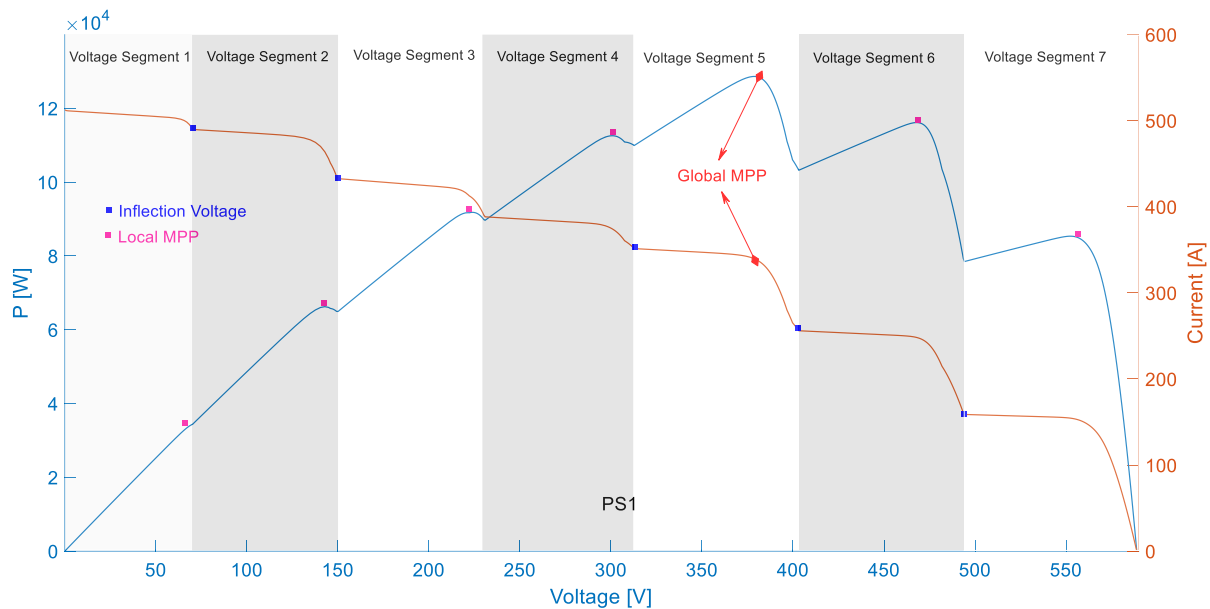


**Figure 1.** Current, voltage, and power values of the PV power system operating under PS1 conditions.

As seen in Figure 1, in a PV power system, depending on the shading conditions, there can be as many voltage levels as the maximum number of panels connected in series. At each of these voltage levels, there is a maximum power point. However, only one of these points is the maximum power point of the PV system, which is called the Global MPP. The others are referred to as Local MPPs. MPPT methods aim to find the Global MPP point as quickly as possible and with the lowest error. Algorithms based on  $0.8V_{oc}$ , which are extensively used in traditional algorithms, determine the MPP point in each voltage segment. In the second stage, the maximum power value obtained from these points is determined, and the system is operated at this point. However, panel data are required to apply this method. In a very recent study, a voltage scanning method was proposed to eliminate this disadvantage in standalone PV systems [34]. Accordingly, the system voltage starting point is determined, scanned up to the system voltage, and power values are recorded. The voltage at the highest power value is defined as the reference voltage. The system is operated at the reference voltage point with the help of a controller. Thus, MPPT is performed independently of PV system parameters. However, various harmonics, resulting from inverter switching in grid-connected PV power systems and large changes in voltage measurements, will lead to errors. Therefore, in this study, a two-stage hybrid MPPT algorithm suitable for use in large-scale grid-connected PV systems was proposed. To test the proposed algorithm, six different partial shading conditions were created. The irradiance values in the shading conditions are shown in Figure 2.

The P-V curves corresponding to six different shading conditions are shown in Figure 3. Accordingly, different scenarios have been created for each voltage region where an MPP will occur. Particularly, the PS3 condition, occurring at the lowest voltage level, presents a challenging characteristic for MPPT algorithms. At the same time, the conditions under PS4 have been the subject of many different studies as complex PSCs. The performance of the proposed algorithm was tested under all these challenging conditions.

	PS1			PS2			PS3			PS4			PS5			PS6			W/m <sup>2</sup>
	1..29	30..58	59..87	1..29	30..58	59..87	1..29	30..58	59..87	1..29	30..58	59..87	1..29	30..58	59..87	1..29	30..58	59..87	
1	1000	850	750	1000	1000	400	800	1000	400	1000	100	500	200	100	1000	200	100	1000	
2	900	1000	900	1000	1000	400	800	1000	400	800	100	500	200	100	1000	200	100	1000	
3	800	1000	900	700	1000	400	400	100	100	800	100	500	200	100	400	200	100	400	
4	700	900	650	700	100	100	400	100	100	800	900	850	200	100	400	200	100	400	
5	600	750	650	200	100	100	400	100	100	800	900	850	400	500	700	400	500	700	
6	500	550	400	200	100	100	200	100	100	500	900	850	400	500	700	400	500	700	
7	400	300	200	200	100	100	200	100	100	500	750	850	400	500	700	400	500	700	

Figure 2. Irradiance values in the PV system operating under six different shading conditions.

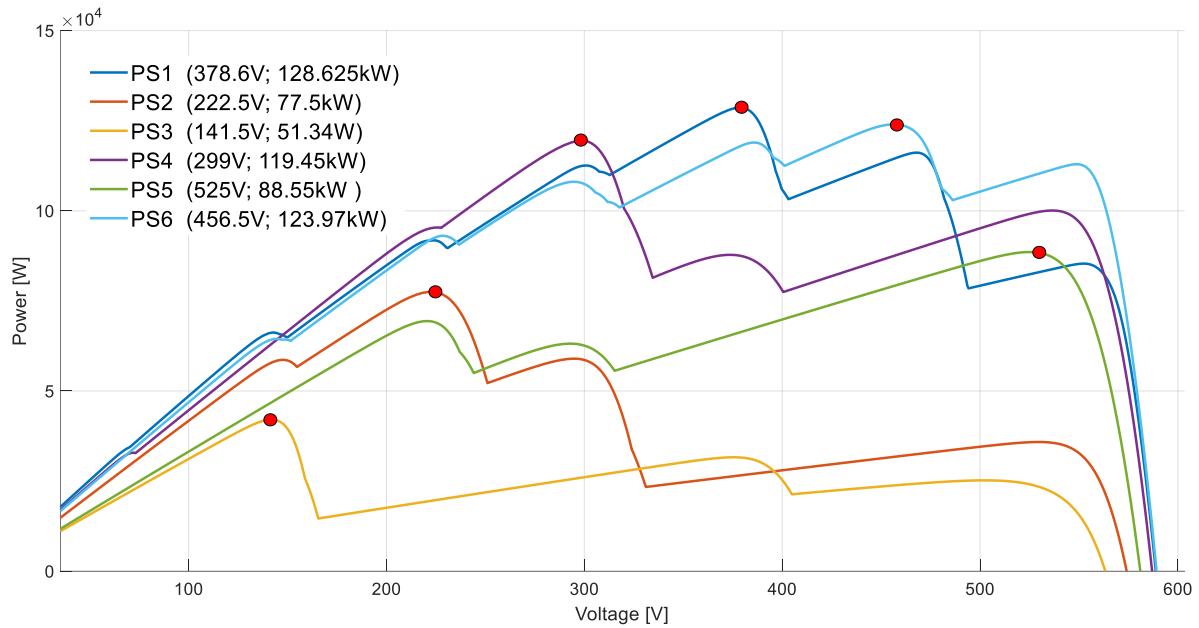


Figure 3. P-V curves under six different partial shading conditions.

The PV system was integrated with a three-phase grid in a MATLAB/Simulink environment to evaluate the proposed method’s effectiveness. As shown in Figure 4, the PV system is connected to a three-phase inverter through a DC-DC boost converter. The voltage reference generated by the MPPT algorithm controls the PV system’s output voltage via a PI controller. The converter parameters are  $C_s = 50 \mu\text{F}$ ,  $C_f = 54,000 \mu\text{F}$ , and  $L_f = 5 \text{mH}$ , and it operates with a switching frequency of 5 kHz.

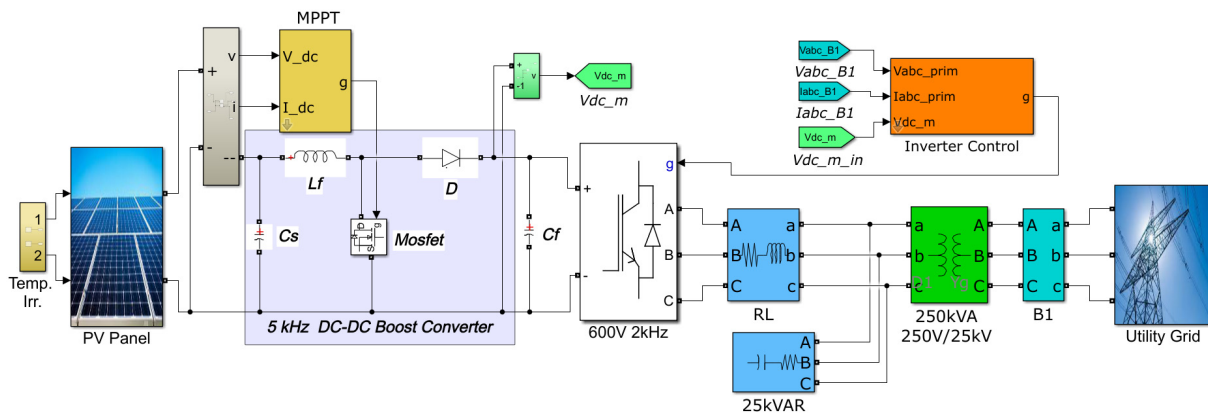


Figure 4. Model of grid-connected PV power system in MATLAB/Simulink.

The simulation of the grid-connected PV system was performed in MATLAB/Simulink. The inverter has a switching frequency of 2 kHz and is linked to the transformer through an output filter. The inverter control is executed in two stages. Initially, the DC-link voltage is monitored, and the active  $I_d$  and reactive  $I_q$  components of the current are obtained. In the second stage,  $V_d$  and  $V_q$  reference voltages are derived from these currents. By comparing these with the mains voltage,  $V_{abc\_ref}$  is obtained, and PWM signals are generated to switch the inverter.

### 3. The Proposed MPPT Algorithm

In the voltage scanning algorithm, the voltage of the PV system is controlled by a PI controller and set to a determined voltage reference. For this, the voltage reference is increased, starting from a certain starting point. The rate of increase should not be faster than the control response. If the reference is increased too quickly, the power calculation may be incorrect at some points. The expression for the linearly increased voltage reference is seen in Equation (6).

$$V_{lnr}(i) = V_{lnr}(i-1) + V_{DD} \quad (6)$$

where  $V_{DD}$  represents the amount of voltage increase, and  $V_{lnr}(i)$  represents the value of the linearly increasing voltage.  $(i-1)$  represents the voltage level at the previous iteration. The voltage increase continues until it reaches the input voltage value of the inverter, thus limiting the voltage increase. While the reference voltage increase continues, the current and voltage values of the PV system are measured, the changes in current, voltage, and power are calculated, and the duty cycle  $D$  at the output of the PI controller is recorded. In the next step, for the maximum power point to be determined, the duty cycle and power values at points where the following equation conditions are met are sampled.

$$\left. \begin{array}{l} \left| \frac{\Delta P}{\Delta V} \right| < 0.001 \\ \& \\ \Delta I > 0.002 \\ \& \\ \Delta P < 0.001 \end{array} \right\} = \begin{cases} V_{mpp} = V_{PV} \\ P_{mpp} = P_{PV} \\ D_{mpp} = D \end{cases} \quad (7)$$

The sampled values are compared with the previous value until the reference voltage  $V_{inv\_dc}$  is reached, and the largest value is determined as  $P_{mpp}$ . The values at this point are assigned as global values, and the voltage value  $V_{mpp}$  and duty cycle  $D_{mpp}$  are determined. At this point, the system is operated for a while with the  $V_{mpp}$  value as the reference voltage. When the reference voltage reaches  $1.2 * V_{inv\_dc}$ , the current duty cycle is assigned as the initial duty cycle  $D_{intr}$ , and the second stage of the hybrid MPPT is initiated. Figure 5a shows the flowchart for the VSC-conventional P&O algorithm. It shows the sequential steps involved in scanning the voltage and perturbing the operating point to track the maximum power point (MPP) of a photovoltaic (PV) system. Figure 5b illustrates the flowchart for the VSC-variable-step P&O, and Figure 5c that for the VSC-modified P&O algorithm. Accordingly, the traditional P&O method is one of the oldest MPPT algorithms known in the literature and is widely used. The VS P&O algorithm used in Figure 5b [5] is a fast and widely used MPPT algorithm in the literature, obtained by adding the value obtained by multiplying the change in  $\left| \frac{\Delta P}{\Delta V} \right|$  by a coefficient  $M$  to the duty cycle increase value, as seen in Equation (8).

$$D(i) = D(i-1) \pm M * \left| \frac{\Delta P}{\Delta V} \right| \quad (8)$$

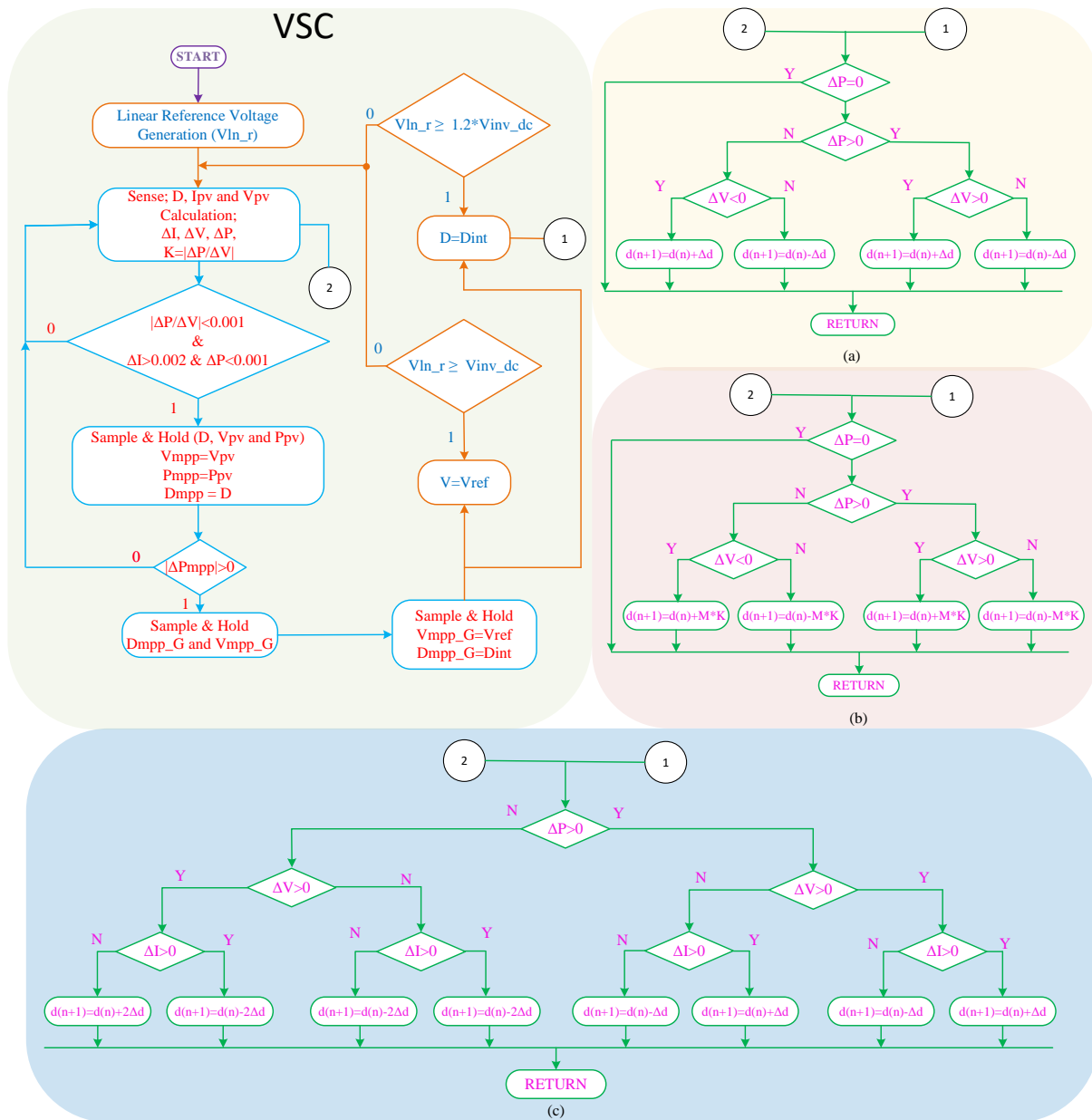


**Figure 5.** Hybrid MPPT algorithms: (a) voltage scanning and traditional P&O; (b) voltage scanning and variable-step P&O; and (c) voltage scanning and modified P&O.

The modified P&O algorithm seen in Figure 5c [15] stands out in the literature as a highly efficient and simple algorithm. In this algorithm, in addition to the traditional P&O algorithm, changes in current are also utilized, taking advantage of both voltage and current changes. When current changes are examined, four more conditions are added differently from the traditional method. Thus, it is determined whether the change in power is due to radiation value or voltage change. If there is a power change due to radiation change, the increase in duty cycle is twice as much, thus preventing deviations from the maximum power point.

#### 4. Simulation Results

In the simulation study, six different PS conditions were run in three different scenarios, and in each scenario, three different PS conditions were run in sequence with different arrangements. Thus, the performance of the algorithms under different conditions was observed. Figure 6 shows the power values obtained in Scenario 1. Accordingly, after the

voltage scanning process in the PS1 condition, the voltage region where the maximum power occurs was approximately determined. In the second stage, three different P&O methods were applied. It was observed that the speed of reaching steady state was higher in the VSC-P&O and VSC-VS\_P&O methods, and the power fluctuations in steady state were lower in the VSC-M\_P&O method. When the PS condition changes, the algorithm starts scanning again, and the same processes are repeated in sequence. In Scenario 1, the second PS condition was determined as PS6. In this condition, the time to reach steady state and the amount of power fluctuation were seen to be approximately the same. In the third PS condition, PS2, the superiority of the proposed method, VSC-M\_P&O, in terms of time to reach steady state and the amount of power fluctuation, is clearly seen.

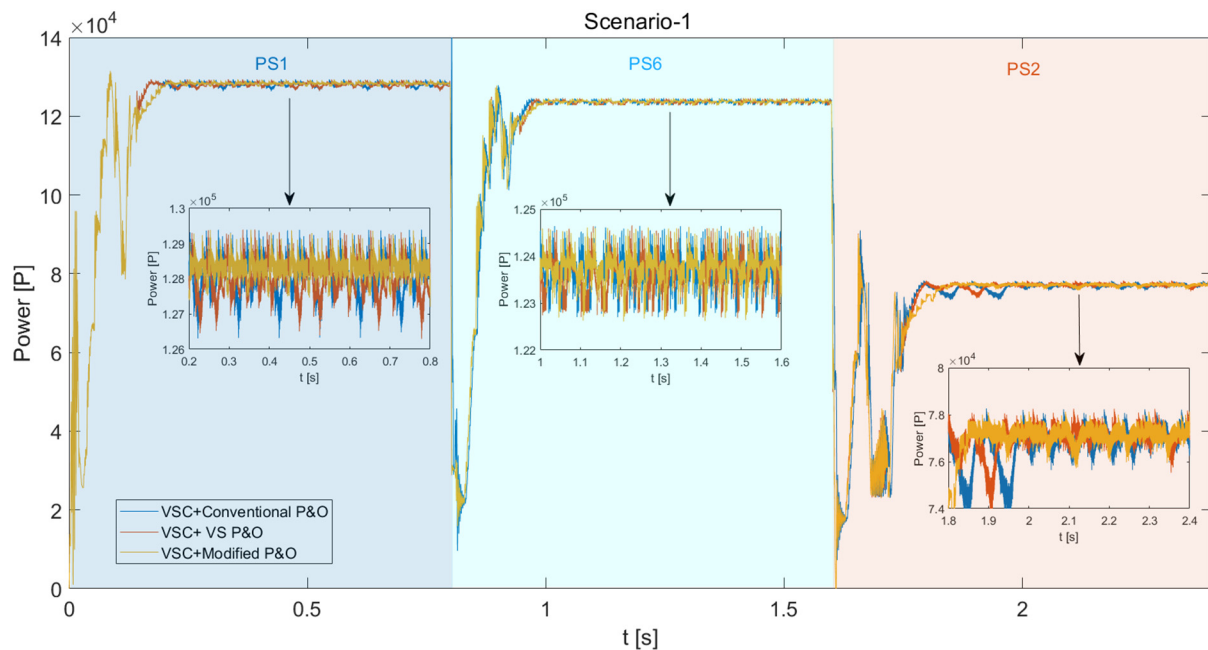


**Figure 6.** Power values obtained from three different methods in Scenario 1 of the PV system.

As seen in Figure 7, Scenario 2 was obtained by sequentially running the PS1, PS2, and PS3 conditions. Accordingly, the PS1 condition has the same values as seen in scenario 1. In the PS2 condition, the VSC-P&O method took longer to reach steady state compared to the other two methods. Although the power fluctuations in steady state were approximately the same, the VSC-VS\_P&O method deviated from steady state for a very short period. In the PS3 condition, despite the proposed method taking longer to reach steady state, it provided a significant advantage in power fluctuation. On the other hand, due to large power fluctuations, the VSC-VS\_P&O method rescanned.

In Scenario 3 (Figure 8), under the PS6 condition, the proposed method took a little longer to reach steady state, but it had a very slight advantage in power fluctuations in steady state. In the PS5 condition, all three methods reached steady state at approximately the same times. However, there was a temporary increase in power fluctuations in steady state for the VSC-P&O and VSC-VS\_P&O methods. While operating under PS4 conditions, although there were delays in reaching steady state with the proposed method, it was observed that the power fluctuations were significantly lower compared to the other two methods.

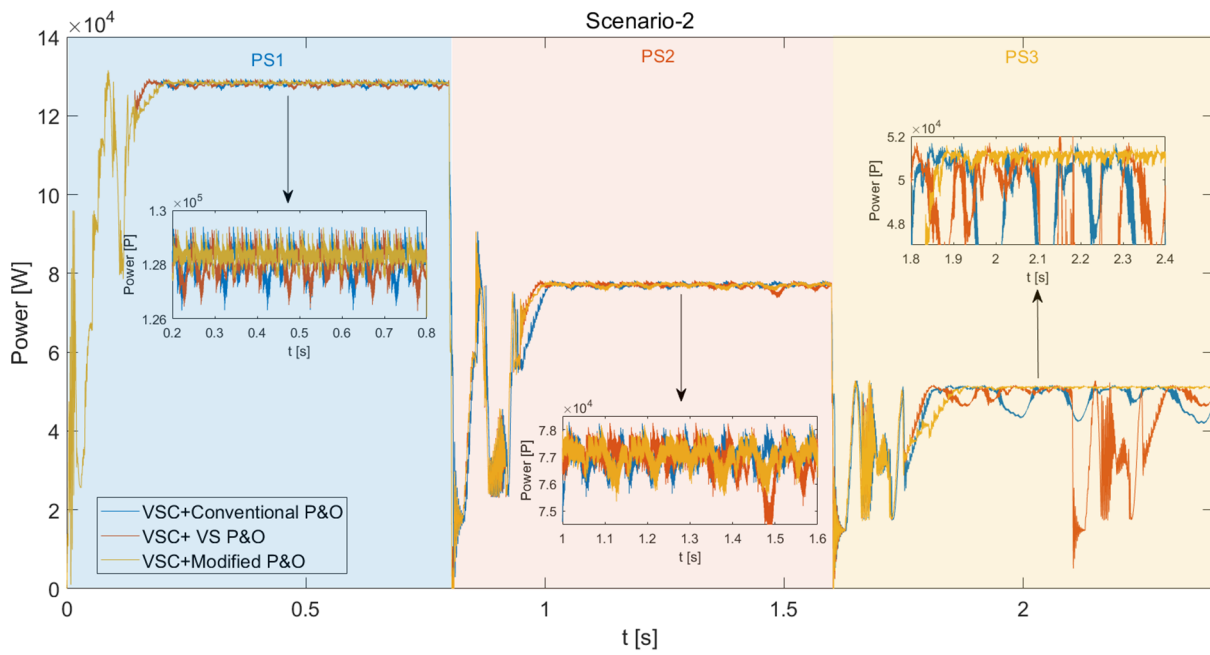


Figure 7. Power values obtained from three different methods in Scenario 2 of the PV system.

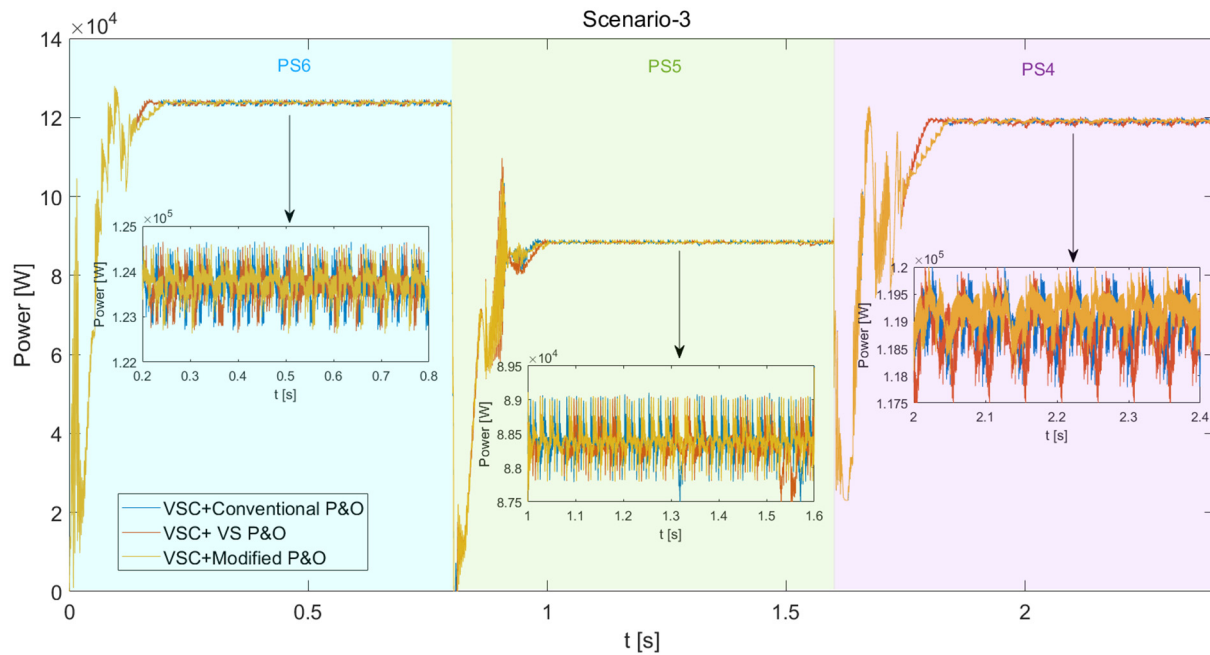
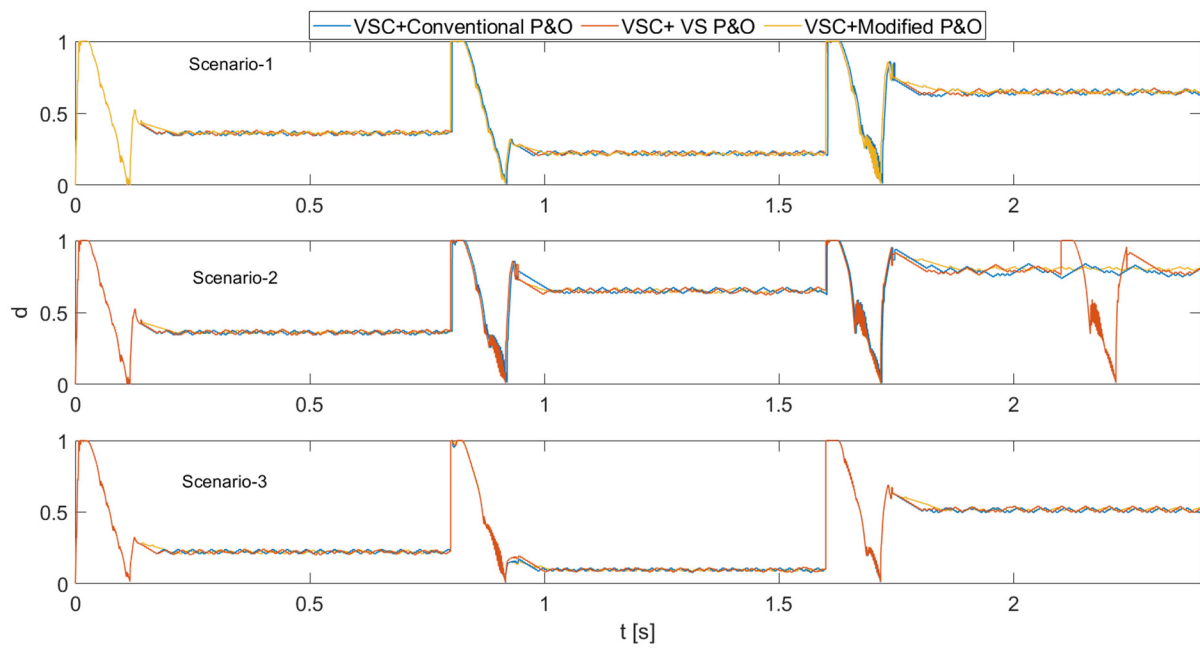


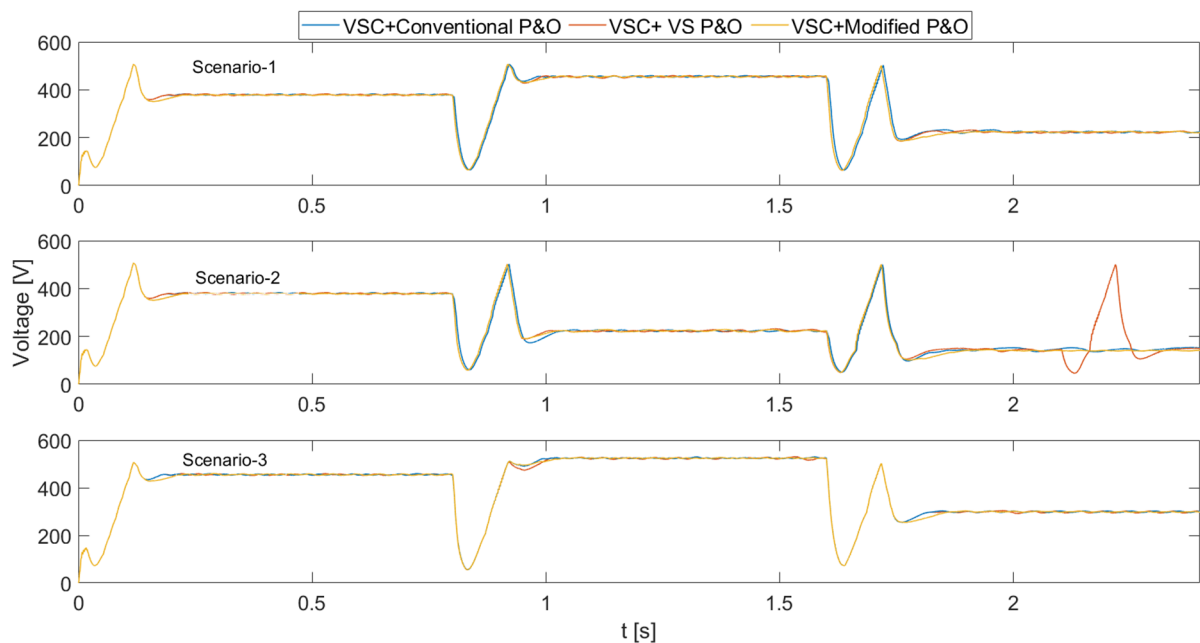
Figure 8. Power values obtained from three different methods in Scenario 3 of the PV system.

Figure 9 displays the duty cycles generated in all three scenarios. Here, the duty cycles formed by the scanning process and subsequently by three different P&O methods can be observed for each PS condition.

Figures 10 and 11 show the voltage and current values generated in all scenarios in the PV system.



**Figure 9.** Duty cycles obtained in all scenarios in the PV system.



**Figure 10.** Voltages obtained in all scenarios in the PV system.

Table 2 presents the tracking speeds, MPPT efficiencies, and power fluctuations in steady state obtained from the simulation study. As seen from the table, the proposed algorithm had a slightly higher tracking speed compared to other algorithms. However, it stood out with lower voltage fluctuations in steady state. In the challenging condition of PS3, other algorithms did not reach a stable power value. On the other hand, when examining MPPT efficiency, it was as efficient as the other methods in all conditions, and in some cases, it was observed to have a higher MPPT efficiency.

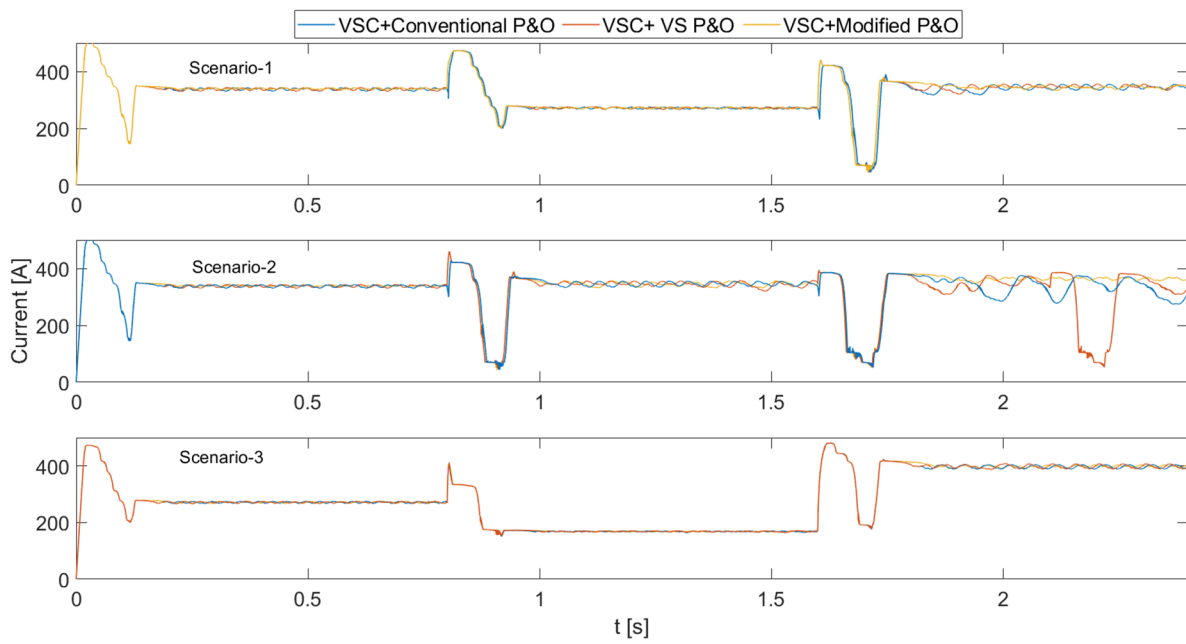


Figure 11. Currents obtained in all scenarios in the PV system.

Table 2. Tracking speed, efficiency, and power fluctuations obtained in all scenarios.

		MPPT Method	Track. Speed (s)	MPPT (%)	Power (kW)	Ripple (kW)
Scenario 1	PS1 (128.625 kW)	VSC-P&O	0.17	99.51	128	3
		VSC-VS_P&O	0.17	99.51	128	3
		VSC-M_P&O	0.19	99.9	128.5	1.5
	PS6 (123.97 kW)	VSC-P&O	0.165	99.66	123.55	1.8
		VSC-VS_P&O	0.17	99.66	123.55	1.8
		VSC-M_P&O	0.18	99.66	123.55	1.8
	PS2 (77.5 kW)	VSC-P&O	0.38	99.67	77.25	2.98
		VSC-VS_P&O	0.38	99.67	77.25	1.85
		VSC-M_P&O	0.25	99.67	77.25	1.5
Scenario 2	PS1 (128.625 kW)	VSC-P&O	0.17	99.51	128	3
		VSC-VS_P&O	0.17	99.51	128	3
		VSC-M_P&O	0.19	99.9	128.5	1.5
	PS2 (77.5 kW)	VSC-P&O	0.2	99.67	77.25	2.1
		VSC-VS_P&O	0.17	99.67	77.25	4
		VSC-M_P&O	0.17	99.67	77.25	2.1
PS3 (51.34 kW)	VSC-P&O	0.2	-	-	-	
	VSC-VS_P&O	0.2	-	-	-	
	VSC-M_P&O	0.25	99.72	51.2	1.15	
Scenario 3	PS6 (123.97 kW)	VSC-P&O	0.17	99.66	123.55	1.8
		VSC-VS_P&O	0.17	99.66	123.55	1.8
		VSC-M_P&O	0.185	99.66	123.55	1.8
	PS5 (88.5 kW)	VSC-P&O	0.17	99.94	88.5	1.55
		VSC-VS_P&O	0.17	99.94	88.5	1.55
		VSC-M_P&O	0.17	99.94	88.5	1.1
	PS4 (119.45 kW)	VSC-P&O	0.2	99.79	119.2	2.1
		VSC-VS_P&O	0.2	99.79	119.2	2.8
		VSC-M_P&O	0.24	99.79	119.2	1.7

In addition to comparing the proposed VSC-M\_P&O algorithm with VSC-P&O and VSC-VS\_P&O, it is important to evaluate its performance against other optimization methods related to P&O and VSC techniques. Various optimization methods have been developed to enhance the efficiency and effectiveness of MPPT algorithms in PV systems. These include the Fractional Short-Circuit Current (FSCC) method, Incremental Conductance (IncCond) method, Model Predictive Control (MPC), Fuzzy Logic Control (FLC), Artificial Neural Network (ANN)-based methods, and Extremum Seeking Control (ESC). Comparing VSC-M\_P&O with these methods would provide a comprehensive assessment of its capabilities in maximizing power generation and minimizing power fluctuations under partial shading conditions, thus contributing to the advancement of MPPT techniques in PV systems.

## 5. Conclusions

This study contributes to the ongoing efforts to enhance MPPT algorithms for PV systems operating under partial shading conditions. The developed hybrid algorithm, combining voltage scanning with a modified P&O method, offers a promising solution with its simplicity, efficiency, and speed. Unlike many existing methods, the proposed algorithm does not require detailed panel data, making it more practical and adaptable. The comparative analysis against traditional methods reveals the superior performance of the VSC-M\_P&O algorithm, particularly in minimizing power fluctuations and maximizing power generation under partial shading scenarios. Hybrid MPPT algorithms have found their place in the literature with their high performance. However, they are generally difficult and complex methods to implement because they often involve optimization or machine learning-based algorithms [39].

In this study, a simple, highly efficient, and high-speed hybrid MPPT algorithm was developed. The proposed algorithm consists of a combination of voltage scanning and a modified P&O method. The voltage scanning algorithm does not require panel data such as voltage, current, and the number of panels. This feature makes it superior to voltage segmentation and  $0.8V_{oc}$  algorithms. The voltage scanning algorithm was used together with traditional P&O, variable-step P&O, and modified P&O algorithms. To test the proposed algorithm, a grid-connected PV power system with a capacity of 252.6 kW was created in the MATLAB/Simulink environment. Data obtained from running six different PS conditions in three different scenarios in this PV power system were compared. Accordingly, the VSC-M\_P&O proposed algorithm stood out in almost all scenarios with low power fluctuations in steady state. Moreover, it was able to generate more power in some PS conditions compared to other methods. A disadvantage of the proposed method is that it had a slight delay in reaching steady state compared to other methods. Future work will focus on reducing this delay and developing modifications to the P&O method so that it can operate faster than other algorithms.

**Funding:** This research received no external funding.

**Institutional Review Board Statement:** Not applicable.

**Informed Consent Statement:** Not applicable.

**Data Availability Statement:** Data are contained within the article.

**Conflicts of Interest:** The author declares no conflict of interest.

## References

1. Celikel, R.; Boztas, G.; Aydogmus, O. A system identification-based MPPT algorithm for solar photovoltaic pumping system under partial shading conditions. *Energy Sources Part A Recovery Util. Environ. Eff.* **2022**, *44*, 5199–5214. [[CrossRef](#)]
2. Gani, A.; Sekkeli, M. Experimental evaluation of type-2 fuzzy logic controller adapted to real environmental conditions for maximum power point tracking of solar energy systems. *Int. J. Circuit Theory Appl.* **2022**, *50*, 4131–4145. [[CrossRef](#)]
3. Çelikel, R.; Gündoğdu, A. Comparison of PO and INC MPPT methods using FPGA in-the-loop under different radiation conditions. *Balk. J. Electr. Comput. Eng.* **2021**, *9*, 114–122. [[CrossRef](#)]

4. Saravanan, S.; Babu, N.R. Maximum power point tracking algorithms for photovoltaic system—A review. *Renew. Sustain. Energy Rev.* **2016**, *57*, 192–204. [[CrossRef](#)]
5. Pandey, A.; Dasgupta, N.; Mukerjee, A.K. High-performance algorithms for drift avoidance and fast tracking in solar MPPT system. *IEEE Trans. Energy Convers.* **2008**, *23*, 681–689. [[CrossRef](#)]
6. Ahmed, J.; Salam, Z. A modified P&O maximum power point tracking method with reduced steady-state oscillation and improved tracking efficiency. *IEEE Trans. Sustain. Energy* **2016**, *7*, 1506–1515.
7. Li, C.; Wen, J.R.; Wan, J.; Taylan, O.; Fei, C.W. Adaptive directed support vector machine method for the reliability evaluation of aeroengine structure. *Reliab. Eng. Syst. Saf.* **2024**, *246*, 110064. [[CrossRef](#)]
8. Ahmed, J.; Salam, Z. An improved perturb and observe (P&O) maximum power point tracking (MPPT) algorithm for higher efficiency. *Appl. Energy* **2015**, *150*, 97–108.
9. Abdelsalam, A.K.; Massoud, A.M.; Ahmed, S.; Enjeti, P.N. High-performance adaptive perturb and observe MPPT technique for photovoltaic-based microgrids. *IEEE Trans. Power Electron.* **2011**, *26*, 1010–1021. [[CrossRef](#)]
10. Killi, M.; Samanta, S. Modified perturb and observe MPPT algorithm for drift avoidance in photovoltaic systems. *IEEE Trans. Ind. Electron.* **2015**, *62*, 5549–5559. [[CrossRef](#)]
11. Zhu, Y.; Kim, M.K.; Wen, H. Simulation and analysis of perturbation and observation-based self-adaptable step size maximum power point tracking strategy with low power loss for photovoltaics. *Energies* **2018**, *12*, 92. [[CrossRef](#)]
12. Belkaid, A.; Colak, I.; Kayisli, K. Implementation of a modified P&O-MPPT algorithm adapted for varying solar radiation conditions. *Electr. Eng.* **2017**, *99*, 839–846.
13. Belkaid, A.; Colak, I.; Kayisli, K. A novel approach of perturb and observe technique adapted to rapid change of environmental conditions and load. *Electr. Power Compon. Syst.* **2020**, *48*, 375–387. [[CrossRef](#)]
14. Ahmed, J.; Salam, Z.; Kermadi, M.; Afrouzi, H.N.; Ashique, R.H. A skipping adaptive P&O MPPT for fast and efficient tracking under partial shading in PV arrays. *Int. Trans. Electr. Energy Syst.* **2021**, *31*, e13017.
15. Ahmed, J.; Salam, Z. An enhanced adaptive P&O MPPT for fast and efficient tracking under varying environmental conditions. *IEEE Trans. Sustain. Energy* **2018**, *9*, 1487–1496.
16. Ait Ayad, I.; Elwarraki, E.; Baghdadi, M. Intelligent perturb and observe based MPPT approach using multilevel DC-DC converter to improve PV production system. *J. Electr. Comput. Eng.* **2021**, *2021*, 6673022. [[CrossRef](#)]
17. Restrepo, C.; Yanéz-Monsalvez, N.; González-Castaño, C.; Kouro, S.; Rodriguez, J. A fast converging hybrid mppt algorithm based on abc and p&o techniques for a partially shaded pv system. *Mathematics* **2021**, *9*, 2228.
18. Hua, C.C.; Zhan, Y.J. A Hybrid Maximum Power Point Tracking Method without Oscillations in Steady-State for Photovoltaic Energy Systems. *Energies* **2021**, *14*, 5590. [[CrossRef](#)]
19. Farzaneh, J. A hybrid modified FA-ANFIS-P&O approach for MPPT in photovoltaic systems under PSCs. *Int. J. Electron.* **2020**, *107*, 703–718.
20. Çelik, Ö.; Teke, A. A Hybrid MPPT method for grid connected photovoltaic systems under rapidly changing atmospheric conditions. *Electr. Power Syst. Res.* **2017**, *152*, 194–210. [[CrossRef](#)]
21. Mohammed, S.S.; Devaraj, D.; Ahamed, T.I. A novel hybrid maximum power point tracking technique using perturb & observe algorithm and learning automata for solar PV system. *Energy* **2016**, *112*, 1096–1106.
22. Mohanty, S.; Subudhi, B.; Ray, P.K. A grey wolf-assisted perturb & observe MPPT algorithm for a PV system. *IEEE Trans. Energy Convers.* **2016**, *32*, 340–347.
23. El-Helw, H.M.; Magdy, A.; Marei, M.I. A hybrid maximum power point tracking technique for partially shaded photovoltaic arrays. *IEEE Access* **2017**, *5*, 11900–11908. [[CrossRef](#)]
24. Lian, K.L.; Jhang, J.H.; Tian, I.S. A maximum power point tracking method based on perturb-and-observe combined with particle swarm optimization. *IEEE J. Photovolt.* **2014**, *4*, 626–633. [[CrossRef](#)]
25. Sher, H.A.; Murtaza, A.F.; Noman, A.; Addoweesh, K.E.; Al-Haddad, K.; Chiaberge, M. A new sensorless hybrid MPPT algorithm based on fractional short-circuit current measurement and P&O MPPT. *IEEE Trans. Sustain. Energy* **2015**, *6*, 1426–1434.
26. Figueiredo, S.; e Silva, R.N.A.L. Hybrid mppt technique pso-p&o applied to photovoltaic systems under uniform and partial shading conditions. *IEEE Lat. Am. Trans.* **2021**, *19*, 1610–1617.
27. Balaji, V.; Fathima, A.P. Hybrid algorithm for MPPT tracking using a single current sensor for partially shaded PV systems. *Sustain. Energy Technol. Assess.* **2022**, *53*, 102415. [[CrossRef](#)]
28. Latifi, M.; Abbassi, R.; Jerbi, H.; Ohshima, K. Improved krill herd algorithm based sliding mode MPPT controller for variable step size P&O method in PV system under simultaneous change of irradiance and temperature. *J. Frankl. Inst.* **2021**, *358*, 3491–3511.
29. Liu, Y.H.; Chen, J.H.; Huang, J.W. Global maximum power point tracking algorithm for PV systems operating under partially shaded conditions using the segmentation search method. *Sol. Energy* **2014**, *103*, 350–363. [[CrossRef](#)]
30. Başoğlu, M.E. An enhanced scanning-based MPPT approach for DMPPT systems. *Int. J. Electron.* **2018**, *105*, 2066–2081. [[CrossRef](#)]
31. Başoğlu, M.E. An improved 0.8 V OC model based GMPPT technique for module level photovoltaic power optimizers. *IEEE Trans. Ind. Appl.* **2018**, *55*, 1913–1921. [[CrossRef](#)]
32. Jatelly, V.; Bhattacharya, S.; Azzopardi, B.; Montgareuil, A.; Joshi, J.; Arora, S. Voltage and current reference based MPPT under rapidly changing irradiance and load resistance. *IEEE Trans. Energy Convers.* **2021**, *36*, 2297–2309. [[CrossRef](#)]
33. Kesilmiş, Z.; Karabacak, M.A.; Aksoy, M. A novel MPPT method based on inflection voltages. *J. Clean. Prod.* **2020**, *266*, 121473. [[CrossRef](#)]

34. Celikel, R.; Yilmaz, M.; Gundogdu, A. A voltage scanning-based MPPT method for PV power systems under complex partial shading conditions. *Renew. Energy* **2022**, *184*, 361–373. [[CrossRef](#)]
35. Ostadrahimi, A.; Mahmoud, Y. Novel Spline-MPPT Technique for Photovoltaic Systems under Uniform Irradiance and Partial Shading Conditions. *IEEE Trans. Sustain. Energy* **2021**, *12*, 524–532. [[CrossRef](#)]
36. Lyden, S.; Galligan, H.; Haque, M.E. A Hybrid Simulated Annealing and Perturb and Observe Maximum Power Point Tracking Method. *IEEE Syst. J.* **2021**, *15*, 4325–4333. [[CrossRef](#)]
37. Zhang, W.; Zhou, G.; Ni, H.; Sun, Y. A Modified Hybrid Maximum Power Point Tracking Method for Photovoltaic Arrays under Partially Shading Condition. *IEEE Access* **2019**, *7*, 160091–160100. [[CrossRef](#)]
38. Kermadi, M.; Salam, Z.; Ahmed, J.; Berkouk, E.M. A High-Performance Global Maximum Power Point Tracker of PV System for Rapidly Changing Partial Shading Conditions. *IEEE Trans. Ind. Electron.* **2021**, *68*, 2236–2245. [[CrossRef](#)]
39. Fei, C.W.; Han, Y.J.; Wen, J.R.; Li, C.; Han, L.; Choy, Y.S. Deep learning-based modeling method for probabilistic LCF life prediction of turbine blisk. *Propuls. Power Res.* **2024**, *13*, 12–25. [[CrossRef](#)]

**Disclaimer/Publisher’s Note:** The statements, opinions and data contained in all publications are solely those of the individual author(s) and contributor(s) and not of MDPI and/or the editor(s). MDPI and/or the editor(s) disclaim responsibility for any injury to people or property resulting from any ideas, methods, instructions or products referred to in the content.